XVIII International Conference on Water Resources
CMWR 2010
J. Carrera (Ed)

CO_2 TRAPPING IN SLOPING AQUIFERS: HIGH RESOLUTION NUMERICAL SIMULATIONS

Maria T. Elenius*, Hamdi A. Tchelepi† and Klaus Johannsen††

*††University of Bergen, Department of Mathematics, BCCS
Thormøhlensgate 55, 5008 Bergen, Norway
e-mail: maria.elenius@uni.no, web page: http://www.uib.no/math
e-mail: klaus.johannsen@uni.no, web page: http://www.uib.no/math

†Stanford University, Department of Energy Resources Engineering
367 Panama Street, Stanford, CA 94305-2220, USA
e-mail: tchelepi@stanford.edu, web page: http://www.pangea.stanford.edu/ERE

Key words: Geological CO_2 sequestration, high resolution simulations, solubility trapping, residual trapping

Summary. We performed numerical simulations of the migration of a supercritical CO_2 current in a sloping aquifer in the presence of residual and solubility trapping. Compared to simulations with residual trapping only, when dissolution is accounted for the trapping efficiency is nearly doubled and the speed and maximum up-dip extent of the plume are affected. The saturations in the plume correspond well to transition zones consistent with capillary equilibrium. The pressure gradients slightly ahead of the leading tip of the current remain at the initial values, and that opens up the possibility to use a simple moving boundary to model extremely long aquifers.

1 INTRODUCTION

Geological sequestration of carbon dioxide (CO_2) has been suggested as a greenhouse gas mitigation strategy[1]. Many of the available storage sites are deep saline aquifers with small dip angles. In these long, thin storage sites, the fate of the CO_2 plumes is determined by competition between the up-dip movement of the lighter and less viscous supercritical CO_2 phase and several trapping mechanisms. The evolution of gravity currents during the post-injection period has been studied by Hesse et al.[2], who developed a semi-analytical sharp interface model that employs a simple model for residual trapping. Pruess et al.[3] performed numerical simulations with upscaling of the convective enhancement of CO_2 mass transfer to the water phase. We perform fully coupled simulations to study the long post-injection period, where the gravity current of supercritical CO_2 competes with both residual and solubility trapping. The objective is to resolve the physics associated with

these coupled nonlinear processes. The fully coupled simulation results can be eventually used to design simplified models that capture the essential features of the evolution.

2 PROBLEM DEFINITION

We model the evolution of a supercritical-CO_2 plume in a deep aquifer that is 30 km long and 50 m thick. The formation, which has an impermeable cap-rock, has a 1 % (0.45°) dip. The governing equations and the initial- and boundary conditions are described in the next two sections.

2.1 Governing equations

The problem is modeled as a two-component, two-phase, compositional problem. The governing equations are mass conservation of each component $C \in \{H_2O, CO_2\}$

$$\partial_t \sum_\alpha \phi S_\alpha \rho_\alpha X_\alpha^C \ + \nabla \cdot \sum_\alpha \rho_\alpha X_\alpha^C \mathbf{u}_\alpha = 0, \tag{1}$$

where $\alpha \in \{w, n\}$ denotes the wetting (water) phase and the nonwetting (supercritical) CO_2 phase (hereafter referred to as the gas phase), ϕ is the porosity, which has an average value of 15 %, and S_α and ρ_α denote saturations and densities, respectively. The water density (without dissolved CO_2) varies between 981 kg/m^3 and 986 kg/m^3 and the gas density varies between 715 kg/m^3 and 717 kg/m^3. For the simulations without dissolution, mean values for the densities are used. X_α^C denotes the mass fraction of component C in phase α. The densities and mass fractions are given by a cubic equation of state[4]. The Darcy velocities, $\mathbf{u}_\alpha$, are given by

$$\mathbf{u}_\alpha = -\frac{k_{r\alpha} k}{\mu_\alpha}(\nabla p_\alpha - \rho_\alpha \mathbf{g}), \tag{2}$$

where k is the permeability (100 mD), μ_α are the viscosities (0.35 cP for the water phase and 0.06 for the gas phase), and p_α is the phase pressure. Rock-fluid properties include relations for capillary pressure (P_c, in bars) and relative permeabilities (k_r) and are given by

$$k_{rw} = S_e^4, \tag{3}$$

$$k_{rn} = 0.4(1 - S_e^2)(1 - S_e)^2 - C, \tag{4}$$

$$P_c = 0.2/\sqrt{(S_e)}, \tag{5}$$

where S_e is the effective water saturation defined as $(S_w - S_{wr})/(1 - S_{wr})$ and C is a constant such that k_{rn}= 0 for $S_n = S_{nr}$. The residual saturations for gas and water are 0.2. There is a vertical temperature gradient of 25 °C/km.

2.2 Initial and boundary conditions

In order to focus on the long post injection period, we worked with a simple initial condition. This also facilitates comparison with analytical models that require relatively simple initial plume shapes. The CO_2 plume initially occupies a rectangular box at the lower end of the aquifer and is separated from the resident water by a sharp straight interface, see figure 2. The simulations are initialized with $2 \cdot 10^7$ kg of gas at residual water saturation in the down-dip part of the aquifer; the rest of the domain is fully saturated with water. The initial pressures are consistent with gravity equilibrium within each region.

Due to capillarity, and because the two regions have differing pressure gradients, the pressures will initially have a discontinuity at the interface between the CO_2 and resident-water phases. The pressures at either side of the interface are such that gas flows up-dip across the interface, which is balanced by down-dip water flow. The difference between the water-pressure in the water and gas regions at a height y above the bottom of the aquifer is shown in figure 1 and is given by

$$\delta(y) = \lambda_n/\lambda_T(P_c(S_{wr}) - P_c(1)) + \Delta\rho g(H/2 - y), \tag{6}$$

where $\lambda_\alpha = k_{r\alpha}/\mu_\alpha$ are the upstream phase mobilities, and $\lambda_T = \lambda_n + \lambda_w$ is the total mobility. Equation (6) was obtained by integrating the flow across the interface, assuming that the velocities are directed along the (sub)-horizontal direction and that the gas and water pressure gradients do not change direction at any height y.

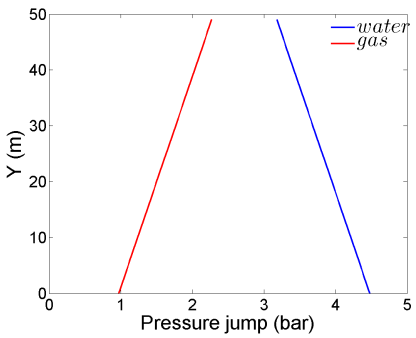

Figure 1: Initial difference between upstream and downstream pressures for the gas and water phases. Note that the water phase has higher pressure jumps, which is required due to the lower mobility. Also note that the pressure jump, and hence velocity, for gas is highest at the top of the aquifer and for water it is highest at the bottom.

Hydrostatic pressure is applied for the up-dip (right) boundary. All other boundaries are closed.

3 NUMERICAL TREATMENT

The General Purpose Research Simulator (GPRS[4,5]) from Stanford University was used to perform high resolution numerical simulations for the model problem. We used a finite-volume space discretization that is first order accurate for transport and second order for pressure. A fully implicit (Backward Euler) first-order approximation is used for time. The nonlinear system was solved with the Newton method and the linear sub-problems were solved with GMRES (Generalized Minimal Residual Method), using the CPR preconditioner (Constrained Pressure Residual[5–7]) with true IMPES decoupling.

4 RESULTS

Simulations were performed using isotropic gridblocks of 9,600, 38,400 and 153,600 cells respectively, with corresponding cell sizes of 12.5 m, 6.25 m and 3.125 m. We first study a case without CO_2 dissolution, and then we study how the results change with dissolution. After that, the sensitivity with respect to the grid is discussed.

4.1 Gravity-current evolution: no dissolution (ND)

Within a short period from the initial placement of the plume, the interface between the gas and water regions gets divided into two separate sections, see figure 2. Between the top of the aquifer and a distance $h \approx 20$ m from the top, there is an advancing portion with buoyancy driven drainage of gas in the up-dip direction. Below this point, there is a receding portion with imbibition of water in the down-dip direction due to buoyancy and capillarity.

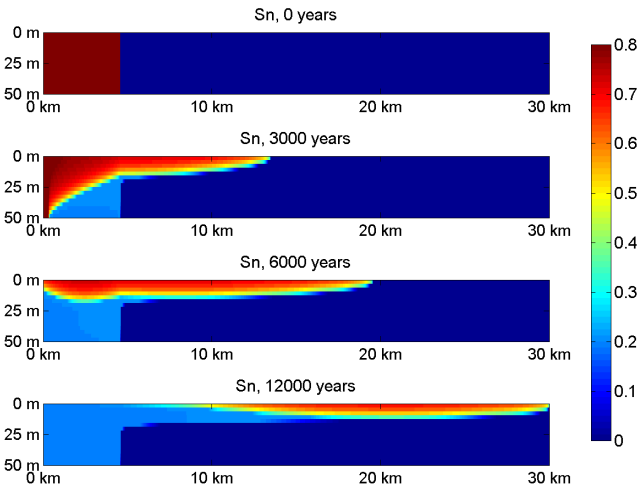

Figure 2: Gas phase saturation.

The receding tip reaches the back end of the initial gas region at the bottom of the aquifer after 3,000 years (the 'transition time' , figure 3), then travels upwards and reaches the top of the aquifer after about 7,000 years. At this point in time, the back-end of the gravity current starts to advance at a constant speed, leaving residual CO_2 behind. The advancing tip speed slows down slightly until the end of a transition period, and then it reaches a constant value of 2.0 m/year. Under these conditions, the advancing tip reaches the up-dip boundary after 12,000 years, and at this time, 37 % of the gas is residually trapped (figure 4).

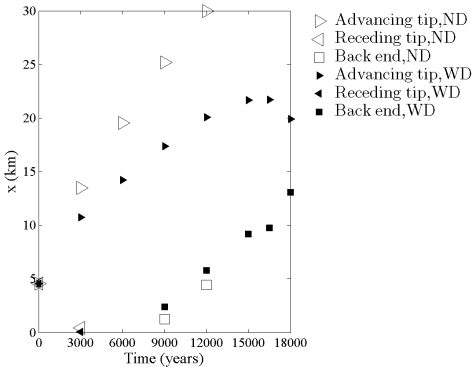

Figure 3: Location of the advancing tip, receding tip, and back end of the current.

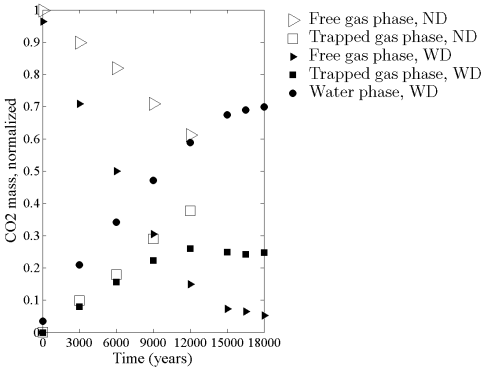

Figure 4: Distribution of CO_2 mass normalized by the total initial CO_2 mass.

At small distances just ahead of the leading tip of the gravity current, the water

pressures remain at the initial hydrostatic gradient.

4.2 Gravity-current evolution: with dissolution (WD)

We now study the evolution when dissolution is accounted for. First, note from figure 4 that the current is almost fully depleted (i.e., no mobile CO_2 plume) when dissolution is accounted for. Figure 3 shows that also in the case with dissolution, the speed decreases with time to reach a constant value after a transition period. However, in the presence of dissolution, the speed decreases more rapidly compared with the ND case to reach a constant value of 1.1 m/year. After about 10,000 years, the advancing tip begins to slow down. The maximum up-dip extent is 22 km and is reached after 17,000 years.

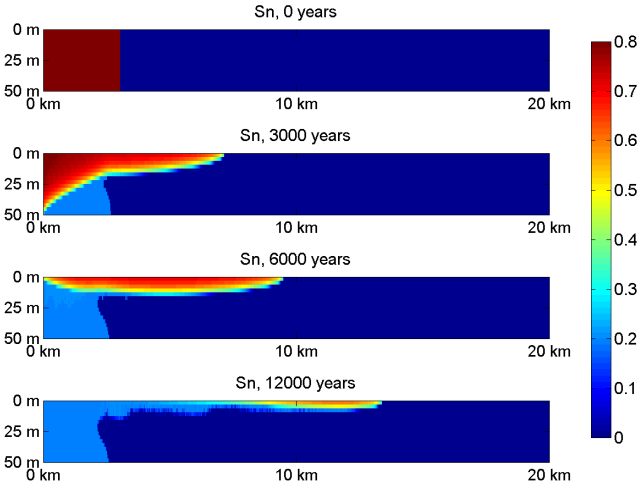

Figure 5: Gas phase saturation with dissolution.

The saturations within the plume correspond well to transition zones consistent with capillary equilibrium, where there is a drainage process.

In the parts of the aquifer where a gas phase is present, the concentration of CO_2 in the water phase is at the solubility limit, which leads to a density increase of 1 % compared to initial water. Further dissolution occurs as the gravity current contacts new water and also due to water exchange across the very elongated interface (transition zone) between the gas and water phases. The latter process occurs with density driven fingering[8] under the current. Fingering begins almost 'immediately' when the plume arrives (figure 6).

Molecular diffusion is not included in the simulations and does not contribute to CO_2 mass transfer across the interface. However, the levels of numerical diffusion associated with the computations are expected to be larger than the those of molecular diffusion.

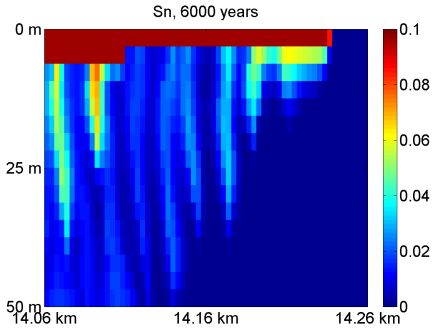

Figure 6: Mass fraction of CO_2 in the water at the front of the current.

4.3 Grid comparison

For the simulations without dissolution, the maximum extent after 9,000 years is 1 % increased with the medium refined grid and 5 % reduced with the coarse grid compared to the fine grid. The reduction for the coarse grid is primarily because the minimum thickness of the plume is bounded by the vertical grid resolution, leading to lower gas saturations for the coarse grid.

For the simulations with dissolution, the maximum extent that the plume reaches before it recedes is 17 % increased with the medium refined grid and 9 % increased with the coarse grid, compared to the fine grid. The lack of a trend is probably due to two counteracting effects. First, numerical diffusion slows down the current. Second, we also think that increased numerical diffusion delays the onset of convection and reduces the overall mass transfer of CO_2 into the water phase, which can increase the speed of the current.

5 SUMMARY AND REMARKS

We used fully coupled simulations to study the long post-injection period, where the evolution of a gravity current of supercritical CO_2 competes with residual and solubility trapping.

Compared to simulations with residual trapping only, when dissolution is accounted for the trapping efficiency is nearly doubled, the speed of the current is halvened, and the maximum up-dip extent of the current is reduced. The results therefore indicate that dissolution must be accounted for in order to obtain first-order estimates regarding the evolution of the gravity current. The fact that the speed is affected by dissolution may call for the need to resolve the onset of density driven fingering.

For the given model problem, the saturations within the plume correspond well to the values obtained by capillary equilibrium, where there is a drainage process.

The pressure gradients slightly ahead of the advancing front of the current remain at

the initial values. The efficiency of numerical tools for the study of CO_2 gravity currents can therefore be improved by using an up-dip boundary that is close to and moving with the same speed as the advancing tip.

Numerical diffusion affects the results, primarily because the thickness of the current is partly controlled by the grid resolution. The results from Hesse et al.[2] predict a speed of 4 m/year for the advancing tip, if there is no capillary transition zone and no dissolution. This is twice the speed of our simulations without dissolution. The difference is partly due to numerical diffusion of our simulations, but probably also due to the capillary transition zone.

Future work will include further grid refinement, inclusion of molecular diffusion, and a study of the parameter space (capillary pressure relations, salinity, permeability etc). We will then make comparison with existing analytical models and make more detailed suggestions for the necessary features of analytical models. We will also perform a linear stability analysis for the onset of fingering in the presence of a capillary transition zone.

REFERENCES

[1] IPCC (Intergovernmental Panel on Climate Change). Special report on carbon dioxide capture and storage. (2005).

[2] M.A. Hesse, F.M. Orr Jr and H.A. Tchelepi. Gravity currents with residual trapping. *J. Fluid Mech.*, **611**, 35–60, (2008).

[3] K. Pruess, J. Nordbotten and K. Zhang. Numerical simulation studies of the long-term evolution of a CO_2 plume under a sloping caprock. *Proceedings, TOUGH Symposium*, (2009).

[4] H. Cao. Development of techniques for general purpose simulators. *Dissertation, Stanford University*, (2002).

[5] Y. Jiang. Techniques for modeling complex reservoirs and advanced wells. *Dissertation, Stanford University*, (2007).

[6] J.R. Wallis. Incomplete Gaussian elimination as a preconditioning for generalized conjugate gradient acceleration. *SPE*, **12265**, (1983).

[7] H. Cao, H.A. Tchelepi, J. Wallis and H. Yardimian. Parallel scalable unstructured CPR-type linear solver for reservoir simulation. *SPE*, **96809** (2005)

[8] A. Riaz, M. Hesse, H.A. Tchelepi and F.M. Orr Jr. Onset of convection in a gravitationally unstable diffusive boundary layer in porous media. *J. Fluid Mech.*, **548**, 87–111, (2006).